The topologically-disordered square lattice

Jean-Marc Greneche, J.M.D. Coey

J. Phys. France **51** (1990) 231-242 1er FÉVRIER **1990**, PAGE 231

Classification
Physics Abstracts
61.40D — 75.25 — 75.50K

The topologically-disordered square lattice

J. M. Greneche ([1], *) and J. M. D. Coey ([2])

([1]) Kernforschungszentrum Karlsruhe, I.N.F.P., Postfach 3640, D-7501 Karlsruhe, F.R.G.
([2]) Department of Pure and Applied Physics, Trinity College, Dublin 2, Ireland

(*Reçu le 19 mai 1989, accepté sous forme définitive le 27 septembre 1989*)

Résumé. — Nous développons la méthode des défauts topologiques à un réseau carré bidimensionnel : la réorganisation topologique obtenue par cassure de liaisons puis création de nouvelles liaisons entre cations, conduit à un système désordonné type AB_2 après insertion des anions. Deux modèles ont été obtenus à partir de défauts topologiques élémentaires de nature différente en tenant compte des contraintes géométriques imposées au cours de leur empilement. Les valeurs de la densité et de l'énergie élastique calculées après relaxation sont plus faibles pour le modèle présentant un nombre plus important de cycles impairs : par ailleurs, des pics de traces cristallines sont observables sur la fonction d'interférence, alors que le second modèle, possédant une majorité de cycles pairs, est typiquement amorphe. Nous présentons la configuration magnétique de l'état fondamental calculée en supposant que toutes les interactions sont antiferromagnétiques et ne dépendent uniquement de l'angle de superéchange ABA.

Abstract. — The topological defect method, consisting of modifying the topology of a crystalline supercell by breaking and reforming bonds between cations, is applied to a two-dimensional square lattice to simulate four-coordinated AB_2 systems after introduction of anions. Two distinct elementary defects are used to generate two highly-disordered networks with geometric constraints imposed on the topological defects. After relaxation, the lower density and lower elastic energy are found for the network with a majority of odd-membered rings which retains vestiges of crystalline peaks in the scattering function $S(q)$; the other network, with a majority of even-membered rings is entirely non-crystalline. Finally, the A-spin configuration in the magnetic ground state, is calculated assuming antiferromagnetic interactions that depend only on the ABA superexchange angle.

Introduction.

The physics of disordered systems has been receiving growing attention during the past two decades. Considerable effort has been devoted to developing structural models, characterizing their topological disorder and evaluating their physical properties. Some concepts have been adapted from crystallography to describe the structure of amorphous materials (amorphography [1]). The idea of frustration [2], used to explain the magnetic behaviour of disordered

(*) Alexander von Humboldt fellow from Laboratoire de Physique des Matériaux, Université du Maine, 72017 Le Mans Cedex, France (*Permanent address*).

systems with antiferromagnetic interactions, was already present in certain crystalline lattices. Such concepts were usually introduced at first for two-dimensional (2-D) systems and then extended to three-dimensions (3-D).

Relatively little attention has been paid to 2-D disordered systems. Besides offering an excellent approach to an understanding of the properties of 3-D disordered systems, they provide a means of interpreting the mechanisms of grain growth in polycrystalline or sintered materials (see Weaire *et al.* [3], physisorption and chemisorption (for a review, see [4]).

To our knowledge, the simplified 2-D Bernal liquid was the first 2-D disordered network discussed in the literature [5] : it was advanced to model the order-disorder transition and consisted of a close-packed assembly of regular or quasi-regular polygons (triangles and squares). An extension of this model, called « the triangular square lattice » was recently discussed in thermodynamic terms [6] ; then a frustrated topology was applied to the problem of amorphous antiferromagnetism assuming Ising [7] and Heisenberg [8] magnetic moments. In an other approach, a 2-D random network, adapted to vitreous silica, was handbuilt by generating arrays of triangles equivalent to extended Zachariasen schematics [9]. Topologically disordered hexagonal networks were obtained by systematically introducing topological defects into a 2-D lattice while respecting boundary conditions [10] : the method consists of breaking and reconnecting bonds, the coordination being kept constant. The author concludes in this paper that the ring statistics converge to fixed values independently of the network size.

In their approach, Weaire and Kermode focused their attention on the evolution of 2-D soap froths [3]. Two processes were introduced to simulate the topological rearrangement of the cells contained in the network so as to reproduce the time evolution of a soap film : one consists of creating a bond and the other of destroying a small cell, the coordination still being kept equal to 3. Their model reproduces well the features observed in soap froth itself, as well as grain growth or plastic deformation in metals [11].

These studies show the interest in understanding the amorphography of 2-D disordered systems. They can also be considered as a first approach to studying real 3-D amorphous materials.

Recently, Wooten and Weaire [12] have developed the topological defect method for generating amorphous tetrahedral structures for a-Si or a-Ge. The procedure involves successive introduction of defects into a large crystalline supercell, each defect resulting in a local rearrangement of the topology, the coordination remaining unaltered.

Our aim is to develop the method for octahedral structures. We have previously analysed two handbuilt structural models [13] and a computed one [14] representing the AB_3 random network composed of corner-sharing AB_6 octahedra. The algorithm for generating the computer model is based on three physical criteria : (i) 6-fold A and 2-fold B coordination, (ii) steric encumbrance of the atoms A and B and (iii) geometrically frustrated topology with the presence of both odd- and even-membered A rings. The latter is indicated by the magnetic behaviour of amorphous FeF_3, where the antiferromagnetic Fe-F-Fe superexchange interactions are frustrated [15].

In this paper, we apply the topological defect method to a 2-D square lattice, thereby generating a planar non-crystalline network. The structure, topology and properties are then discussed. Extension to 3-D will be reported elsewhere [16].

The topological defect method.

We begin with a crystalline square superlattice containing the A positions which was taken to represent the 2-D cation network ; the B anions are placed mid-way between nearest

neighbour A cations. Only four-membered rings are present in such a network. The topological defect method consists in modifying the topology of the starting configuration by breaking some cation-cation bonds and then reforming new cation-cation bonds which respect the coordination. The local rearrangement involved after introduction of two types of defect are illustrated in figure 1. The first topological defect (Fig. 1a) consists in rotating the internal square ring defined by cations A, B, C and D as follows : the BE, CF, DG and AH bonds are broken and then the AE, BF, CG and DH bonds are connected. The second one (Fig. 1b) consists in breaking BC and AD bonds and then reconnecting AC and BD bonds. Defect (1) may be considered as a dislocation quadrupole and defect (2) as a dislocation dipole. The final arrangement in both cases exhibits three and five-membered rings : a six-membered ring can result from the judicious juxtaposition of two topological defects. Furthermore, the topological environment created by one type of defect can be obtained by juxtaposing several of the other ones, and *vice versa.*

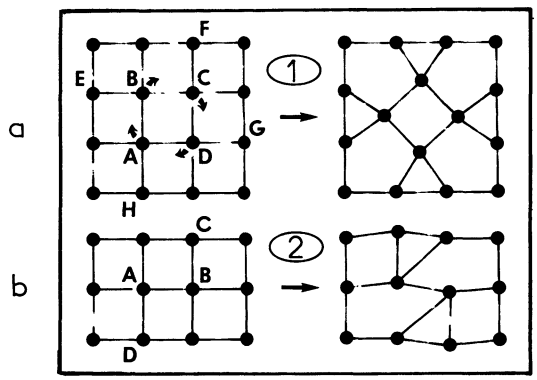

Fig. 1. — Local rearrangement induced by the two types of topological defects discussed in the text.

The locations of the topological defects are chosen randomly by the computer program. Some of the topological defects may be moved to optimize the homogeneity of the disorder. No dangling bonds or double bonds between two cation nearest neighbours are allowed. Some rules relying on geometrical considerations to exclude unrealistic situations were established as explained in next section.

When a topological defect is generated near the outer edge of the square superlattice, the neighbourhood is obtained by consideration of periodic boundary conditions.

The final A-site topology is achieved when no more defects that satisfy the rules can be introduced. At this stage, the anions are inserted by placing the B-atoms mid-way between two cation nearest neighbours. Then, a procedure of structural relaxation using an harmonic potential (analogous to that used in [14]) is extended to the whole model, in conjonction with periodic boundary conditions. The topology is unchanged by such a relaxation procedure. Finally, different physical parameters are deduced from the relaxed structural network : density, radial distribution functions, interference functions, distortion parameters, ring statistics, angular distribution functions, magnetization and spin correlation function (assuming an interaction scheme and allocating a magnetic moments to A ions only).

The geometric problem.

To maintain an analogy with non-crystalline solids where chemical constraints like atomic radius and chemical bond nature exist, the atomic arrangement of the 2-D disordered

structure is not completely random ; a certain regularity is imposed by the local atomic arrangement : consequently, some geometric constraints due to this short-range order have to be taken into account when superimposing the topological defects. The problem, in other words, is how to fill a plane with somewhat distorted polygons, the 4 : 2 coordination being everywhere maintained.

In the present study, the following quantitative limits were established, guided by the structural data observed on the three polymorphic crystalline phases of FeF_3 [17] and those on the amorphous forms [18]. First, the type of polygon is limited to triangle, square, pentagon or hexagon. In addition, the polygons have to be convex and weakly distorted : a concave or a highly-distorted polygon would be equivalent to unrealistic large-angle distortions in the local structure. Then we analysed the different possibilities of filling a plane with polygons so as to establish the rules to be applied in order to avoid unrealistic stituations when superimposing the topological defects : 35 cases are found and only the more favorable ones are listed in table I. The lower and upper limits on the sum of the four ideal angles AAA around one A atom were estimated as follows : first by taking the ratio of A and B ionic radii, one obtain a lower limit for the angle ABA (135°) is appropriate for Fe^{3+} and F^-), and then by considering the lower and upper values of the AB distance experimentally observed (1.95 (3) Å) found for a-FeF_3 [18]. From these data, two extreme values were defined equal to 330° and 385° between which the distortions can be consistent with the structural observed data on the amorphous ferric fluorides. The sum of the four real AAA angles is, of course, 360°.

Table I. — *Geometric situations encountered in a two-dimensional case.*

Ring	3	4	5	6	Σ (*)	Comments
angle value for a regular *n*-ring	60°	90°	108°	120°	—	—
n-ring number through one cation	0	4	0	0	360°	no distortions
	1	2	0	1	360°	
	2	0	0	2	360°	
	1	1	2	0	366°	weak distortions
	1	2	1	0	348°	
	2	0	1	1	348°	
	1	1	1	1	348°	
	0	3	1	0	378°	
	2	0	2	0	336°	
	1	0	3	0	384°	
	1	3	0	0	330°	
	2	1	0	1	330°	
	1	1	0	2	390°	strong distortions
	0	3	0	1	390°	
		and so on				

(*) Σ is the sum of the four ideal angles assuming regular rings through the A cations.

The two 2-D models.

The starting supercell was a square lattice containing 50 × 50 A sites, which should be large enough to be representative of the amorphous state. The distances between two first-nearest neighbours was taken as a. Then the method was applied to generate two models, 1 and 2, using only the defects a and b respectively presented in figure 1. The final topology of the two models is illustrated in figures 2 and 3 : 214 a-type and 269 b-type defects were successfully introduced. One can first remark that no « unrealistic » situation is observable in either model, in agreement with the limits proposed in table I.

In figures 4 and 5, the A-site topology of the two models is presented after carrying out the relaxation procedure on whole system (2 500 A cations and 5 000 B anions) taking into account the periodic boundary conditions. The distance AB was initially taken equal to $a/2$ ($d_{AB} = 1.95$ Å).

Structural analysis of the 2 models.

The ring statistics presented in table II show that the two models are topologically rather different. No six-membered rings were allowed in the second network. The first model contains 64 % of odd-membered rings while the second one contains 44 %. In addition, the elastic energy of the second model is found to be four times higher than that of the first one, after applying the structural relaxation procedure in both cases. At this stage, we conclude that the model with six-membered rings is more realistic.

Table II. — *Ring statistics for the two-dimensional models compared to a no-defect squared lattice.*

	3 %	4 %	5 %	6 %	$\langle n \rangle$
Squared lattice	—	100	—	—	4
Model 1	37	31	28	4	4
Model 2	22	56	22	—	4

The structural characteristics of the two relaxed models are reported in table III. Here it would appear that the two models are very similar, although the AA, AB and BB peaks are broader for the second model. Note also that the density calculated for the model 1 is lower than that of the crystalline phase, while the density of the model 2 is higher ; such changes are directly related to the nature of the topological defects.

In other respects, by looking at the radial distribution functions (RDF) (see for example the AA partial RDF and the total RDF presented in Figs. 6 and 7 respectively), one can conclude that the two models are structurally very different : the first structure model looks like that of a distorted crystalline lattice while the second one exhibits the typical signs of an amorphous structure.

The interference functions $S(q)$ for the no-defect square lattice and for the two models 1 and 2 are shown in figure 8, where it may be seen that vestiges of crystalline Bragg peaks remain in model 1, but they are absent in model 2. Only model 2, based on the dislocation dipole defect, is truely « amorphous ».

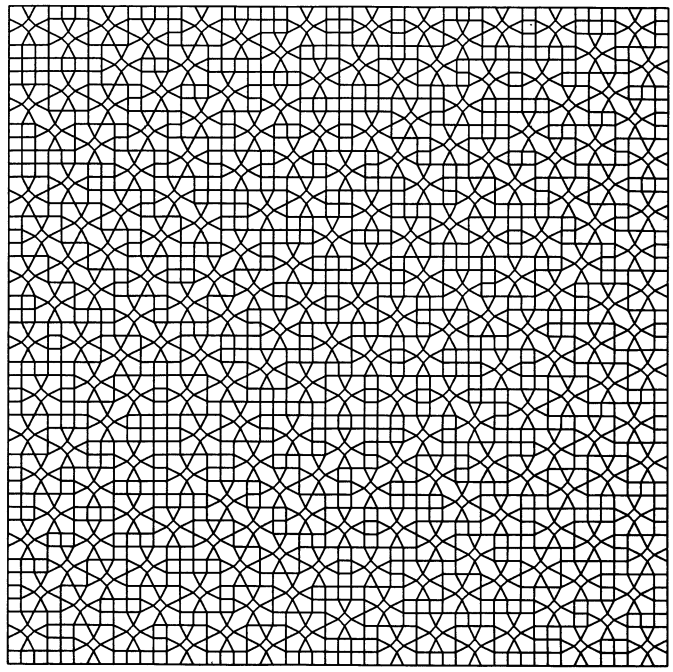

Fig. 2. — Representative view of the square model 1 before applying the structural relaxation procedure.

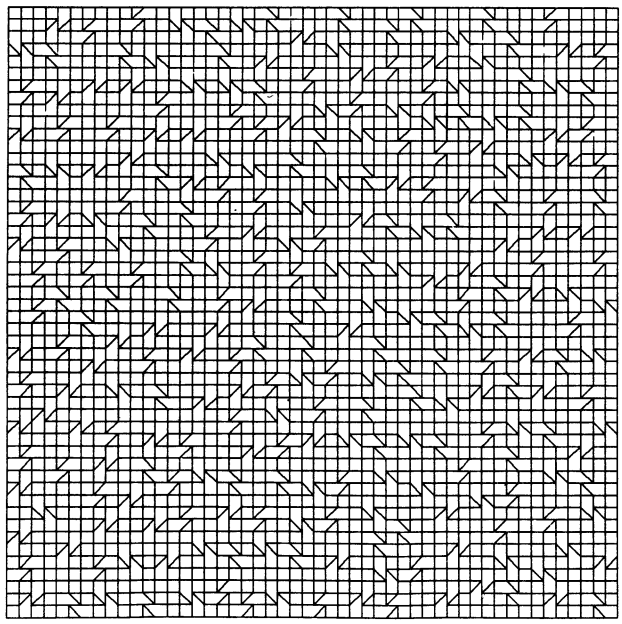

Fig. 3. — Representative view of the square model 2 before applying the structural relaxation procedure.

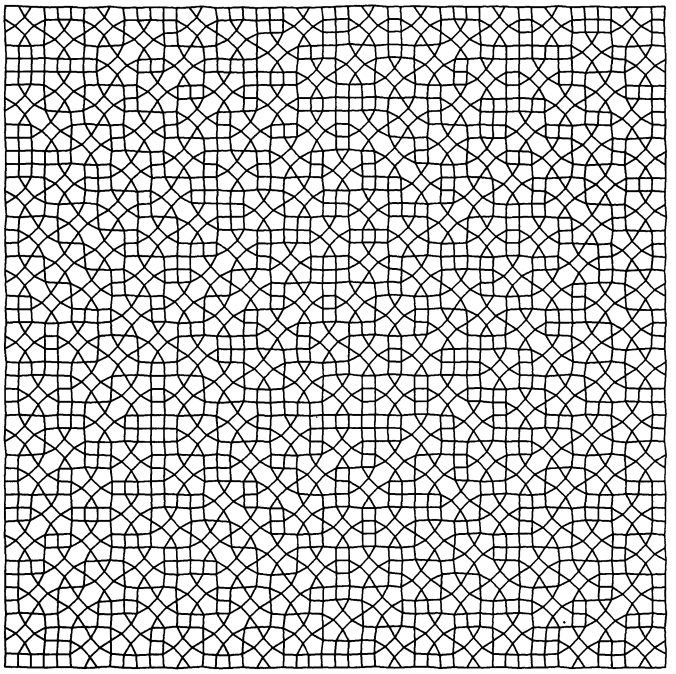

Fig. 4. — Representative view of the square model 1 after applying the structural relaxation procedure.

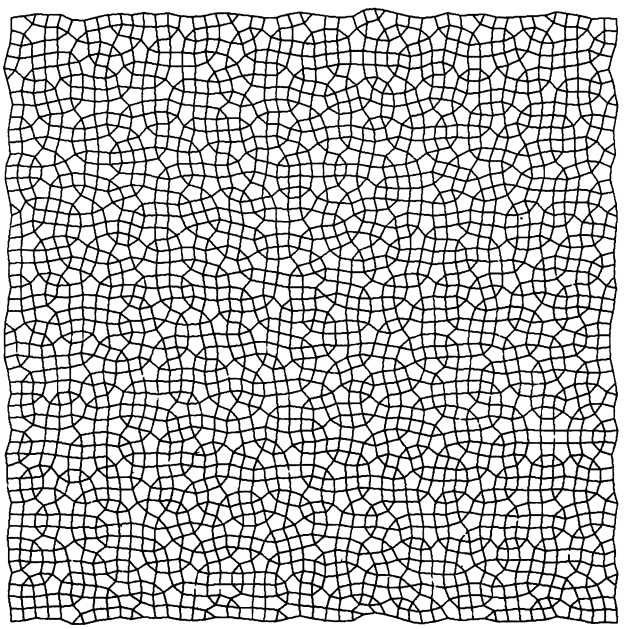

Fig. 5. — Representative view of the square model 2 after applying the structural relaxation procedure.

Table III. — *Structural characteristics of the two-dimensional models compared to the no-defect square lattice* (a = 3.90 Å).

	Surface density	d_{AA} (Å)	d_{AB} (Å)	d_{BB} (Å)	ABA degrees	BBB degrees	BAB degrees	α (*) —	β (*) —
Squared lattice	d_0	3.90	1.95	2.76	180	60	90	0	0
Model 1	0.98 d_0	3.83(19)	1.95(3)	2.76(16)	162(13)	60(9)	90(8)	0.00(1)	− 0.00(1)
Model 2	1.01 d_0	3.83(22)	1.95(9)	2.75(13)	162(13)	60(8)	90(10)	0.00(2)	− 0.00(1)

(*) α and β are the distortion parameters of the AB_2 units

$$\alpha = \sum_1^4 \ell_n \frac{d_{AB}}{d^0_{AB}} \quad \text{and} \quad \beta = \sum_1^4 \ell_n \frac{d_{BB}}{d^0_{BB}} \quad \text{where} \quad d^0_{AB} \text{ and } d^0_{BB}$$

are the equilibrium distance between A and B and two first-nearest B atoms respectively.

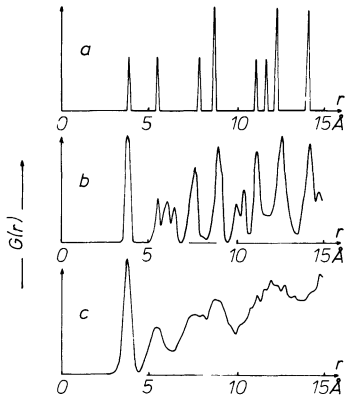

Fig. 6.

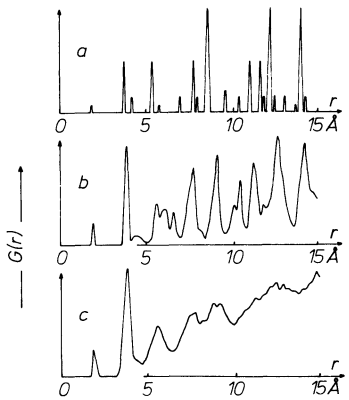

Fig. 7.

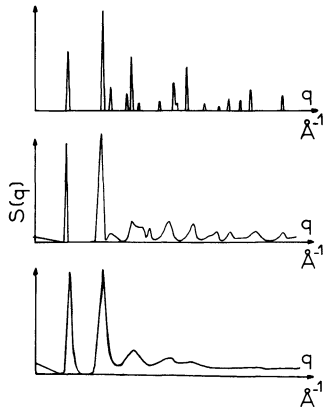

Fig. 8.

Fig. 6. — AA radial distribution functions of a no-defect square lattice (a), of model 1 (b) and of model 2 (c).

Fig. 7. — Total radial distribution functions of a no-defect square lattice (a), of model 1 (b) and of model 2 (c).

Fig. 8. — Interference functions of a no-defect square lattice (a), of model 1 (b) and of model 2 (c).

Magnetic behaviour.

The calculation of the magnetic structure consists of determining the magnetic moment directions after minimizing the energy for classical spins. The initial state with directions of the A site magnetic moments oriented in the plane was randomly generated by the computer for the two models. An XY spin interaction was considered between the 4 nearest neighbours as following,

$$H_{ij} = - \sum_{ij} J_{ij} S_i S_j (\cos A_i B_{ij} A_j)$$

(a)

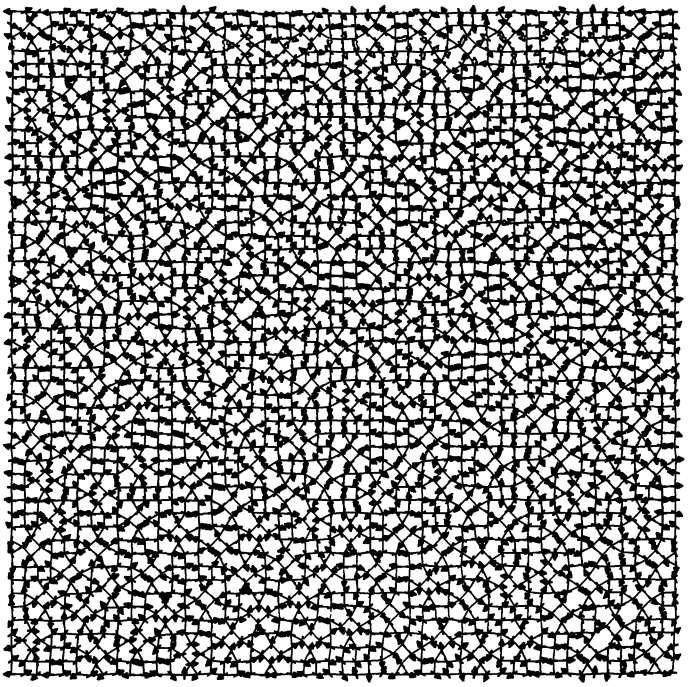

(b)

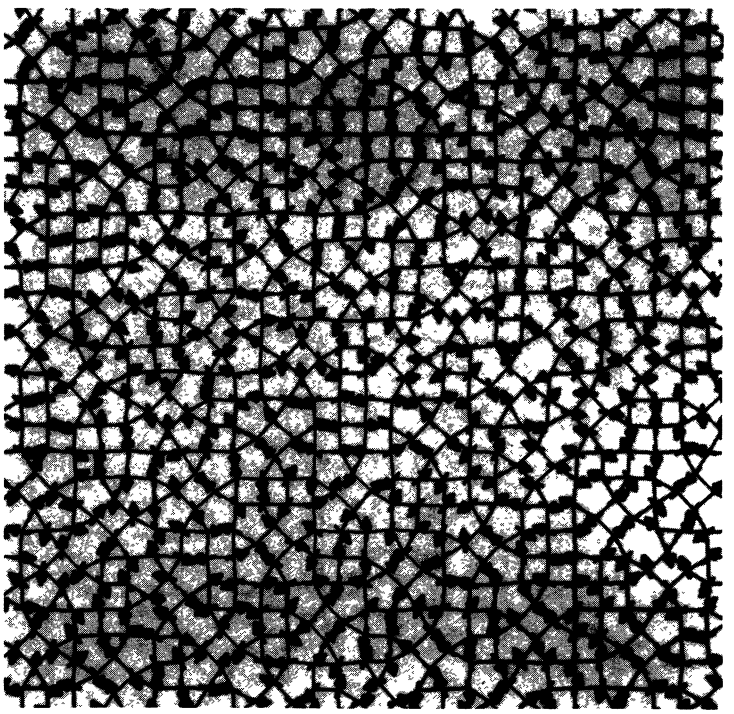

Fig. 9. — Representative view of the magnetic structure of model 1 after applying the magnetic relaxation procedure (a) ; details are given on (b).

(a)

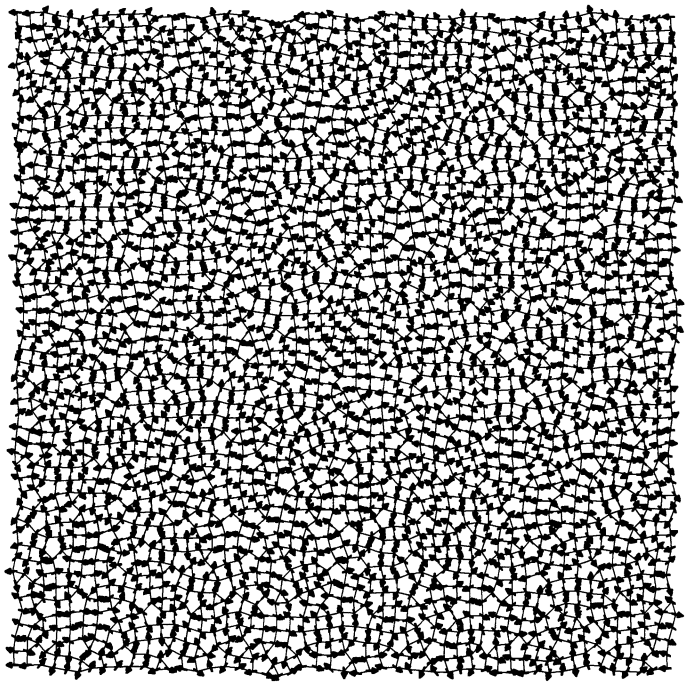

(b)

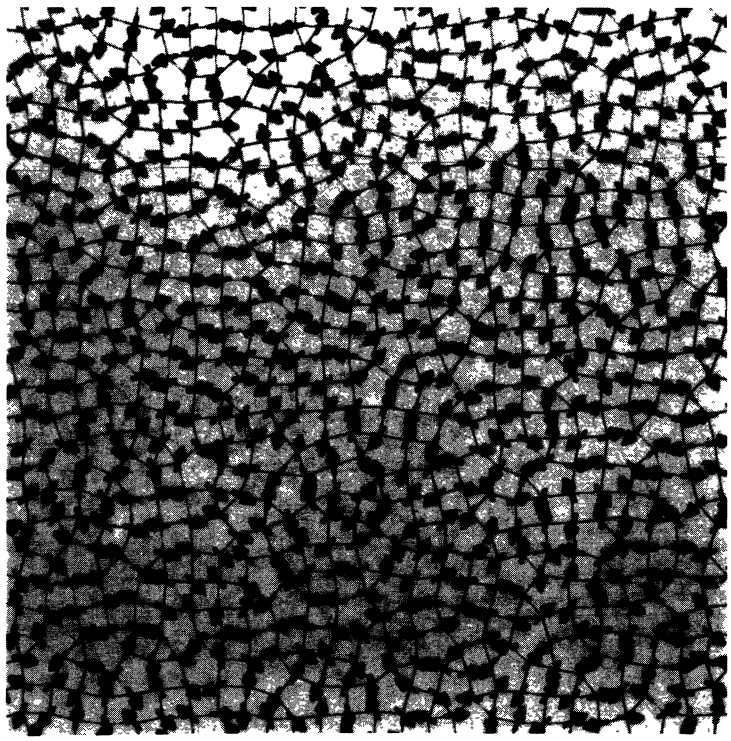

Fig. 10. — Representative view of the magnetic structure of model 2 after applying the magnetic relaxation procedure (a) ; details are given on (b).

where J_{ij} represents the integral exchange coupling (negative in the case of antiferromagnetic interactions) which is related to the superexchange angle ABA but assumed independent of the distance between first-nearest neighbours AA. The magnetic structure is then relaxed by minimizing the magnetic energy according a gradient method which was previously developed for crystalline fluorides [19] : each spin is examined individually and rotated according to the torque due to its magnetic neighbours at each iteration ; in addition the periodic boundary conditions were also taken into account.

The final magnetic configurations are presented in figures 9 and 10 respectively and the magnetic characteristics are reported in table IV. The frustration degree can be estimated from the magnetic energy per spin which appears to be very similar in both cases although their topologies are rather different (see the percentage of odd-membered rings in Tab. IV). In addition, the spin correlation functions were estimated for both models and compared to that of a no-defect antiferromagnetic square lattice, as shown in figure 11.

Table IV. — *Magnetic characteristics of the two-dimensional models compared to the no-defect squared lattice.*

	No-frustrating rings %	Frustrating rings %	⟨sin (ABA)⟩	E_{mag}/spin	M/spin
Squared lattice	100	0	1	$-4J_{AA}$	1
Model 1	35	65	0.86(14)	$-2.36J_{AA}$	0.90
Model 2	56	44	0.86(15)	$-2.53J_{AA}$	0.90

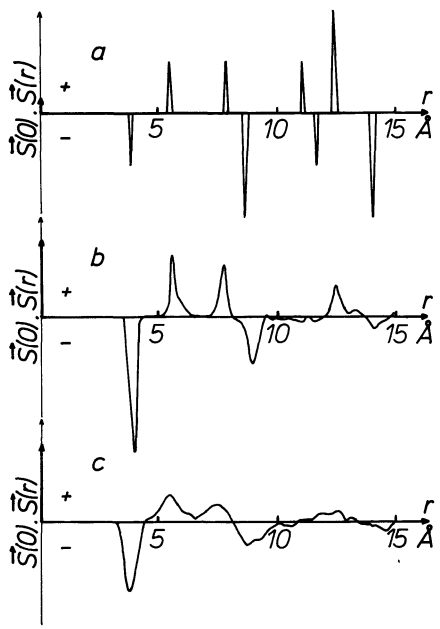

Fig. 11. — Spin correlation functions of a no-defect square lattice (a), of model 1 (b) and of model 2 (c).

The shape of the spin correlation function calculated for the first model confirms that it looks like a distorted crystalline lattice. In both cases, the difference between the A-A radial distribution function (presented in Fig. 6) and the spin correlation function shows that the magnetic moments are isotropically distributed in the plane and indicates an antiferromagnetic coupling between first-nearest magnetic moments.

Conclusions.

The application of the topological defect method to the 2-D square lattice shows that the superimposition of topological defects may lead packing difficulties with physically reasonable atomic sizes. The two 2-D models obtained by generating two types of topological defect subject to plausible geometric constraints are structurally and topologically rather different ; one retains traces of crystalline order, while the other does not but they exhibit similar magnetic behaviour : the magnetic moments are isotropically distributed in the plane.

Acknowledgments.

The authors thank Prof. D. Weaire for stimulating discussions during the present study. One of us (J. M. G.) wishes to thank Dr G. Czjzek and Prof. H. Rietschel for their hospitality in the Kernforschungszentrum of Karlsruhe and for the facility of computing.

References

[1] WRIGHT A. C., in Coherence and Energy transfer in Glasses, Ed. P. A. Fleury and B. Golding, p. 1.
WRIGHT A. C., CORNELL G. A. N. and ALLEN J. W., *J. Non Cryst. Solids* **42** (1980) 69.
[2] TOULOUSE G., *Commun. Phys.* **2** (1977) 115.
VANNIMENUS J. and TOULOUSE G., *J. Phys. C : Solid State Phys.* **10** (1977) L537.
[3] WEAIRE D. and KERMODE J. P., *Philos. Mag. B* **47** (1983) L29 ; *Philos. Mag. B* 48 (1983) 245.
[4] WEAIRE D. and RIVIER N., *Contemp. Physics* **25** (1984) 54 ;
WEAIRE D., Topological Disorder in Condensed Matter, Ed. F. Yonezawa and T. Ninomiya (Berlin : Springer) 1983, p. 51.
[5] COLLINS R., *Proc. Phys. Soc.* **83** (1964) 553.
[6] KAWAMURA H., *J. Magn. Magn. Mater.* **31-34** (1983) 1487 ; *Prog. Theor. Phys.* **70** (1983) 352 ; Topological Disorder in Condensed Matter, Ed. F. Yonezawa and T. Ninomiya (Berlin : Springer) 1983, p. 181.
[7] KAWAMURA H., *Prog. Theor. Phys.* **70** (1983) 697.
[8] KAWAMURA H., *Prog. Theor. Phys.* **73** (1983) 311.
[9] SHACKELFORD J. F. and BROWN B. D., *J. Non Cryst. Solids* **44** (1981) 379 ;
SHACKELFORD J. F., *J. Non Cryst. Solids* **49** (1982) 19.
[10] HE H., *J. Non Cryst. Solids* **94** (1987) 22.
[11] WEAIRE D. and KERMODE J. P., *Philos. Mag. B* **50** (1984) 379.
[12] WOOTEN F. and WEAIRE D., *Solid State Phys.* **40** (1987) 1 and references therein.
[13] COEY J. M. D. and MURPHY P. J. K., *J. Non Cryst. Solids* **50** (1982) 125 ;
GRENECHE J. M., TEILLET J. and COEY J. M. D., *J. Non Cryst. Solids* **83** (1986) 27.
[14] GRENECHE J. M., TEILLET J. and COEY J. M. D., *J. Phys. France* **48** (1987) 1709.
[15] FEREY G., VARRET F. and COEY J. M. D., *J. Phys. C : Solid State Phys.* **12** (1979) L531 ;
GRENECHE J. M., VARRET F., LEBLANC M. and FEREY G., *Solid State Commun.* **63** (1987) 435.
[16] GRENECHE J. M. and COEY J. M. D., to be published.
[17] FEREY G., DE PAPE R., LEBLANC M. and PANNETIER J., *Revue Chim. Minérale* **23** (1986) 474.
[18] GRENECHE J. M., LE BAIL A., LEBLANC M., MOSSET A., VARRET F., GALY J. and FEREY G., *J. Phys. C : Solid State Phys.* **21** (1988) 1351.
[19] LINARES J., GRENECHE J. M. and VARRET F., *J. Phys. Colloq. France* **49** (1988) C8-901.